NBSIR 75-724 (R)

Piezoelectric Polymer Films for Fuze Applications

Philip E. Bloomfield

Electronic Technology Division
Institute for Applied Technology
National Bureau of Standards
Washington, D. C. 20234

August, 1975

Final Report Covering Period
September 1, 1973 to December 31, 1974

Prepared for
U.S. Army Frankford Arsenal
Philadelphia, Pa. 19137

NBSIR 75--724 (R)

PIEZOELECTRIC POLYMER FILMS FOR FUZE APPLICATIONS

Philip E. Bloomfield

Electronic Technology Division
Institute for Applied Technology
National Bureau of Standards
Washington, D. C. 20234

August, 1975

Final Report Covering Period
September 1, 1973 to December 31, 1974

This document has been prepared for the use of the U.S. Army Frankford Arsenal. Responsibility for its further use rests with that agency. The measurement results reported are derived from a statistically small number of specimen devices, and the conclusions that may be drawn are therefore tentative.

Prepared for
U.S. Army Frankford Arsenal
Philadelphia, Pa. 19137

U.S. DEPARTMENT OF COMMERCE, Rogers C.B. Morton, *Secretary*
James A. Baker, III, *Under Secretary*
Dr. Betsy Ancker-Johnson, *Assistant Secretary for Science and Technology*

NATIONAL BUREAU OF STANDARDS, Ernest Ambler, *Acting Director*

ABSTRACT

Described is the development of polymer piezoelectric devices with sufficient electrical output in response to impact to demonstrate the feasibility of using polymer elements in place of ceramic elements in ordnance fuze systems. To satisfy this requirement, piezoelectric polymer elements have been constructed capable of providing at least 0.3 mJ into a 4-Ω load, in response to a force of 89 kN (10 tonsf). Total activities of up to 360 pC/N have been achieved from elements built up from 30 sheets of 25-μm poly(vinylidene fluoride). Test methods developed to characterize both single-sheet and total-element activities are described, as are poling procedures and details of element construction. Mathematical analyses of polymer piezoelectric output into resistive-capacitive loads are presented for static and dynamic cases. Experimental results and theoretical predictions are shown to be in agreement to within the 10% estimate of measurement accuracy.

SYMBOLS USED IN THIS REPORT

A, area

C, polymer capacitance [first defined in appendix A, (10)]

d, piezoelectric strain tensor [with elements d_{nm}]

d_{33}, longitudinal piezoelectric strain constant (an element of d)

D, electric displacement vector [with components D_n]

E, electric field vector [with components E_n]

E, energy delivered to L

E_o, energy parameter [first defined in appendix B, (39)]

δ, function relating E and Y [first defined in appendix B, (40), for triangular force pulse]

F, force vector applied normal to polymer piezoid surface

F_o, applied force amplitude

g, piezoelectric stress tensor [with elements g_{nm}]

g_{33}, longitudinal piezoelectric stress constant (an element of g)

g, function relating E and Y [first defined in appendix B, (59), for haversine force pulse]

i, current

i_G, current generated by P [first defined in appendix A, (13)]

ℓ, polymer thickness

L, electrical load; the subscript "L" denotes that the quantity so modified refers to the electric load; examples: C_L, capacitance of L; R_L, resistance of L; Q_L, charge on C_L; i_L, current through L; V_L, voltage across L.

P, poled active portion of polymer; the subscript "P" denotes that the quantity so modified refers to the polymer P portion as distinguished from the S portion; examples: C_P, capacitance of P; R_P, resistance of P; Q_P, charge on C_P; i_P, current through R_P.

Q, charge

Q_o, open circuit charge [first defined in appendix B, (30)]

R, resistance

S, unpoled shunt portion of polymer; the subscript "S" denotes that the quantity so modified refers to the polymer S portion as distinguished from the P portion; examples: C_S, capacitance of S; R_S, resistance of S; Q_S, charge on C_S; i_S, current through R_S.

t, time

t_o, pulse width of V_L [first defined in appendix B, (44)]

T, piezoelectric stress vector [with components T_m]

V, voltage

V_o, open-circuit voltage [first defined in appendix B, (40)]

Y, the product $\nu\tau$

β, dielectric impermeability tensor [with elements β_{nm}]

ε, dielectric permittivity tensor [with elements ε_{nm}]

ζ, capacitive parameter [first defined in appendix A, (23)]

θ, phase shift in oscillatory component of $V_L = V_L(t)$, for haversine force pulse.

ν, the reciprocal of the circuit decay time [first defined in appendix A, (23)]

τ, pulse half-width of applied force

ϕ, phase shift in oscillatory component of $V_L = V_L(t)$, for half-sine force pulse.

Piezoelectric Polymer Films for Fuze Applications

Philip E. Bloomfield

1. INTRODUCTION

1.1 Objectives

The central objective of this project was to develop polymer devices which would be as effective as the piezoelectric ceramic disks presently used in fuze systems and which would provide low-cost construction, mechanical flexibility, and versatility of electrical arrangement. In order to achieve this goal, it was necessary to increase the outputs of piezoid devices by developing more effective poling and stacking techniques. (The term "poling" refers to the process by which as-received polymer is rendered piezoelectrically active and is described in 2.2. A stack incorporates a sandwich of two or more individual sheets into a single structure, with leads, shields, and the like. The active polymer part of the stack is referred to as a piezoid.) The final goal was the production and delivery of polymer stacks having an electrical output comparable to that of the ceramic discs. This would enable the sponsor to set an achievable standard for piezoid devices to be employed in fuzing systems.

Objectives related to the development and delivery of polymer devices included (1) the development of methods to increase piezoelectric activity, (2) the development of methods to characterize piezoelectric activity under a number of loading conditions, (3) the application of such methods to piezoids developed in the work, and (4) the derivation and formulation of expressions relating piezoid output to applied force.

1.2 Accomplishments

This project was characterized by (1) a growth of understanding of the nature of piezoelectricity in polymers and of the practical difficulties in manipulating fairly large areas of polymer sheet, together with (2) a similar growth of understanding of the differences and similarities between the electrical properties of piezoelectric polymers and piezoelectric ceramics. This improvement in understanding was shared by the NBS staff and the project monitors of Frankford Arsenal through frequency formal and informal contacts.

The initial work statement of July 9, 1973, called for NBS to "fabricate samples and carry out joint experimental studies with the Pitman-Dunn Laboratories, Frankford Arsenal on piezo-polymer films." Shortly after experimental work was begun, it was found that the intended active areas of 30 cm^2 could not be effectively electroded, poled, and stacked by the techniques previously developed and used on smaller areas. With continued improvement in poling procedures, NBS was able to produce sheets with increasingly higher activity. Thus the available energy output per stack was continuously raised over the course of the project and the minimum desirable device figure of merit was raised accordingly by the sponsor. By September, 1974, the characteristics of piezo-polymer stacks delivered

to the sponsor by NBS represented greater activity from a smaller piezoid volume than had originally been considered attainable. Accordingly, the new values were taken by the sponsor as defining goals for any future polymeric devices for the intended test purposes: piezoid stacks with an active area of 30 cm^2 and a maximum thickness of 0.7 mm having a static piezoelectric activity of 280 pC/N and capable of delivering 2000 ergs (2.0×10^{-4} J) into a 4-Ω load in response to a force of 89 kN (10 tonsf) which has a rise time of 10 μs.

With respect to cost goals, at the time of project termination the estimated direct labor cost of producing and testing a sixteen-sheet stack had been brought below $500. This figure applies to laboratory conditions; presumably, the cost would be considerably reduced in mass production.

The development of polymer devices for ordnance fuze applications has resulted in the following specific accomplishments:

1. Development and improvement of poling techniques to achieve piezoelectric activities of 12 picocolombs per newton (pC/N) for a single sheet of poly-(vinylidene fluoride) [PVF_2] 25-micrometers (25-μm) thick, with 14 pC/N realisable on the basis of a 50% success ratio,

2. Development of stacking methodology to achieve a piezoelectric activity of 360 pC/N from a piezoid of 30 sheets of 25-μm PVF_2,

3. Delivery of stacks representative of the current level of activity, (see table 5),

4. Development of a quasi-static, or d-c, method of test to characterize piezoelectric activity of both single sheets and stacks, using a press,

5. Development of a dynamic method of test to characterize piezoelectric activity of both single sheets and stacks, using a drop-test machine,

6. Derivation of an expression relating piezoelectric and pyroelectric activity, so that measurements of either type of activity may be used to characterize the other [1]*,

7. Development of the theoretical basis for a method of test to measure the compliance of bonding layers in a stack [1], and

8. Development of theoretical analyses describing the quantitative behavior of piezoelectric polymer in response to applied force, including derivation of the relationship between electrical and mechanical parameters, and of expressions for optimizing piezoid output into a given electrical load.

---

*Figures in brackets indicate the literature references in section 6.

In developing piezoids with higher levels of energy output, it was necessary to electrode, pole, and test large numbers of single sheets and to assemble and test large numbers of stacks. In the course of this work test methods were developed, discarded, or modified as needed; test equipment was designed, tried, modified, and improved, and many sheets and some stacks were tested to destruction. (As one example, a stack was tested in an air gun at Harry Diamond Laboratories to investigate the ability of a new type of electrical connection to survive violent impact; as another example, several small stacks were destroyed while various bonding agents and techniques were tried in the development of a method to attach leads and glue the poled sheets together.) The understanding and improved techniques derived from this testing program made it possible to achieve the more important of the specific accomplishments listed above.

2. EXPERIMENTAL DEVELOPMENT

2.1 Background

Piezoelectricity in stretched and polarized sheets of PVF_2 was first reported and studied by workers at several Japanese research institutes [2, 3, 4]. Recently, very thin, uniform films of this polymer have become available. Among the advantages of this material are that it has low density, that it is available in sheets (hence devices may be fabricated with surface areas large compared to those of ceramic piezoelectrics), and that it is sufficiently flexible to permit fabrication into a range of shapes. Through the choice of sheet thickness, number of sheets, and electrical connection, a stack may be designed to have specified capacitance and to deliver a maximized electrical output into a given load, in response to an applied force.

At the inception of this project, limited experience was available with active areas as large as 30 cm^2; further, single-sheet piezoelectric elements had been made on what was for the most part a one-at-a-time basis, and there was no developed stacking technology. Thus, new methods and apparatus were required to: (1) extend the vacuum deposition technique to routinely apply metal-film electrodes of 30-cm^2 area, to apply electrodes to one side of a series of polymer elements in quick succession (i.e., without requiring separate pump-down and cycling of the vacuum chamber for each element), and to support the polymer sheet while the electrodes were being applied in such a manner as to minimize the effects from heating (especially wrinkling of the polymer sheet), (2) improve and extend poling procedures to enable the poling of several large samples at once, to utilize higher electric fields and temperatures without introducing wrinkles in the polymer, and to minimize the number of short circuits occurring through the sample during poling, (3) produce a bonded stack from a number of single-sheet elements, and (4) attach leads for parallel electrical connection of the single-sheet elements in a stack.

In addition, methods were required that were appropriate for the tasks of characterizing the piezoelectric activity of single-sheet elements, of sandwiches of elements being built into a stack, and of completed stacks.

2.2 Sample Preparation

2.2.1 Deposition of Electrodes — Aluminum electrodes approximately 0.10-μm thick were deposited on each side of the 25-μm polymer sheets using vacuum evaporation apparatus. Short lengths of the pure aluminum wire used were coiled around a resistively heated tungsten helix; the heating current was not applied until the chamber reached a pressure Of 2.7×10^{-4} pascal (Pa) during pump down.

Polymer surfaces to receive electrodes were rinsed in ethyl or isolpropyl alcohol before being placed in the vacuum chamber. A fixture was designed with two rollers. The polymer sheet to receive electrodes was in the form of a long strip and was initially wound on the feed roller oriented so that when unwound the intended side would face the evaporation apparatus. The take-up roller was driven by means of a mechanical link through a vacuum seal to a crank outside the vacuum chamber. The number of elements that could be produced in one run was limited in principle by the diameter of the rollers and associated clearances; however, in practice the limit was the number of evaporations that would be carried out before more aluminum wire had to be affixed to the tungsten helix.

The electrodes were deposited through a mask which consisted of four circular holes 30 cm^2 in area (diameter = 6.2 cm) in a 24-cm-square sheet of stainless steel. The holes were symmetrically oriented about the center of the mask with a center-to-center spacing of 7.5 cm in one direction (across the roll width) and 8.7 cm in the other (along roll length). Each of these holes had an associated slot, 3 by 12 mm, cut in the mask from the edge of the hole outward along an extension of the hole center line parallel to the intended long axis of the polymer film, with all slots on the same side of the holes. See figure 1. After one side of the polymer sheet strip had electrodes applied, the strip was rewound on the feed roller so as to have been effectively rotated through an angle of 180° (the original "beginning" end wound on the feed roller first) and turned over with former bottom side now top side. The result of the orientations so achieved was successively to evaporate electrode "tails" on opposite sides of the strip pointing in opposite directions. During poling and in subsequent use, electrical connections were made to these projections.

When the electrode thickness is less than 0.07 μm, the resistance across the 30-cm^2 circular face of the electrode, measured from near edge to near edge along a diameter, exceeds 2 Ω. This measurement was made in air using probe tips with a radius of curvature of 1.25 mm. The resulting activity of the poled films is several orders of magnitude less for electrode thicknesses corresponding to resistances greater than 6 Ω than for those corresponding to 2 Ω; the activity was found to be independent of electrode thickness for thicknesses greater than 0.10 μm. (At this thickness, the resistance was near 1 Ω.) If the electrode thickness were permitted to exceed 0.15 μm, the aluminum tended to flake off. An aluminum electrode thickness of 0.1 μm (1000 Å) has proven satisfactory and is recommended. Aluminum was chosen for the electrode material because it is satisfactorily conductive at reasonable thickness, because at such thicknesses it adheres well to alcohol-rinsed PVF_2, and because it is an easy material to evaporate, having a sufficiently low melting temperature not to require the use of a crucible.

2.2.2 Poling — In preparation for poling, a sandwich was made by placing a 125-μm sheet of PVF_2 on a bottom 0.32-cm sheet of polytetrafluoroethylene (PTFE), followed by the electroded polymer element to be poled, another 125-μm sheet of PVF_2, and a top 0.32-cm sheet of PTFE. Electrical connection to the top and bottom electrodes was made by using two thin strips of 12-μm-thick tin foil. This assembly was then placed between the platens of an hydraulic press. A load of approximately 30 kN was applied to press the sample and to prevent it from wrinkling during poling. The desired electrical field was applied across the sample by connecting the tin-foil leads to a high-voltage d-c power supply. The sample was heated to the desired temperature by means of heaters embedded in the platens of the press, and then cooled to room temperature by running water through cooling passages also in the platens. The field was applied to the polymer during the entire heating and cooling cycle. The PTFE served to provide electrical isolation of the sample from the hydraulic press structure. The 125-μm sheets of PVF_2 were used as liners because the surface of the insulating sheets was not smooth. The temperature was monitored by means of thermocouples inserted into the sandwich.

During the assembly of the sandwich, care was taken that the polymer element and the inner sides of the 125-μm PVF_2 were clean and free of dust in order to prevent dirt particles from being pressed into the polymer surface during poling. The thickness of the polymer would be reduced at the embedded particle, and therefore the effective electrical field would be locally high. Embedded particles are to be avoided as potential failure sites.

A regulated 10 kV d-c power supply was used to provide the poling field. The poling voltage typically ranged between 2000 and 2400 V across the 25-μm sheets, with some of the early sheets poled at 1200 V. The 2400 V potential produced a higher activity than did 2000 V, but also resulted in a higher percentage of the sheets failing. For example, the percent success-failure ratio experienced in the laboratory for poling at 2400 V and 120°C was 50-50; for sheets poled at 2000 V and 110°C the percentage of failures dropped to 10. The sheets were heated to approximately 120°C and then cooled. The temperature cycle was approximately 15 min for heating and 10 min for cooling.

2.2.3 Stack Construction — Each poled sheet had a "high side," this being the side with electrodes connected to the positive, or high, side of the d-c poling supply. As the first step in making a multi-sheet stack, two sheets at a time were bonded together, high side to high side, with a tin-foil lead providing electrical contact to the internal high electrodes. Tin-foil leads were attached to the electrode tails with silver-filled rubber paint. Bilaminate pairs were then bonded together with tin-foil leads providing contact to the internal low electrodes and extending from the opposite edge (i.e., 180° away from the edge with high-side leads). Successive high-side leads were aligned one over the other, as were low-side leads. The bonding agent was a solution of one part contact cement to five parts toluene*. Experience with stack construction showed that it was desirable during bonding to prevent entrapment of air bubbles and avoid wrinkling sheets, as both conditions degraded performance.

---

*Considerable experimentation was conducted with various bonding agents. Contact cement meeting Federal Specification MMM-A-130a has been satisfactory.

In the manner described the stack was built up of $2n$ sheets. The partially completed stack had n superposed high-side leads extending from one edge and n - 1 superposed low-side leads extending from the other edge. Two more tin-foil leads were then attached to the outside low-side electrodes. The bundle of high-side leads was bonded to form a single lead with silver-filled rubber paint and reinforced with either copper or aluminum tape. An exterior coat of silver-filled rubber was applied to the reinforced lead. Similar treatment was given to the low-side leads. Figure 2 shows a laminated stack at the bottom (A), before the outer coatings of heavy aluminum tape (providing electrical shielding and mechanical protection) were applied. B shows a single sheet with electrodes deposited on both sides; C shows a similar sheet with one foil electrode attached (which was destined to be an outer low-side lead for the stack); and D shows two sheets bonded together with the high-side lead at the left. E shows another sandwich of two bonded sheets with high-side lead. The laminated stack was made up by alternating D-and-E sandwiches.

2.3 Static Testing Procedure

Each poled sheet separately, and the various small stacks which were an intermediate stage in the fabrication of completed stacks, were tested quasi-statically on an hydraulic press.

When the piezoid sheet or stack is compressed, negative charge collects at the high-side electrode; after discharge, and upon release of the mechanical force, negative charge collects at the low-side electrode. The test procedure was as follows: With an open-circuit configuration, (see figure 3), either the piezoid by itself (with capacitance C) or in parallel electrical connection with a standard capacitor (capacitance C_L) was charged by means of compression or release of pressure (static force loading F_o) by means of the single-pole switch show in the figure. Discharge of the charged piezoid into the preamplifier of a storage oscilloscope permitted measurement on the stored trace of the voltage developed across the capacitor(s).

The magnitude of the charge developed by the polymer is Q_o. The voltage V_o measured when the piezoid is not connected to C_L is Q_o/C.

With C_L in the piezoid circuit, the charge developed Q_o is shared between C_L and C. Under the open-circuit condition there is a common voltage across the two capacitors. In order to obtain a measure of charge output and the quasi-static capacitance of a given piezoid, two voltages, V_o and V_L were measured:

$$V_o = Q_o/C \text{ and}$$

$$V_L = Q_L/C_L = (Q_o - Q_L)/C, \qquad (1)$$

where Q_L and $Q_o - Q_L$ are the equilibrium values of the charge on capacitors C_L and C , respectively. From (1),

$$C = (V_o/V_L - 1)^{-1} C_L, \text{ and } Q_o = CV_o, \qquad (2)$$

From these two formulas and from measurements of V_0 and V_L, the static capacitance C, the charge released Q_0, and the activity Q_0/F_0 may be calculated.

2.3.1 Summary of Single-Sheet and Small-Stack Activities — Presented are data taken from August 28, 1974, through September 14, 1974, while stack No. 7 (30 sheets; see table 5) was being constructed. Four samples in each 15 x 18-cm sheet (as obtained from the vacuum aluminizing apparatus) were poled together in parallel; then each sample in the batch of four was assigned a common batch number and a sample code letter a through d. The active areas were cut apart from each other into four separate single sheets.

Poling voltage (V) and maximum temperature reached during the poling cycle (°C) are given in table 1, along with capacitance C (nF) and piezoelectric activity Q_0/F_0 (pC/N) for eleven batches. C and Q_0/F_0 are the averages of the measured values for the four samples in each numbered batch. Both quantities were obtained by measurement and calculation using (2) for applied forces up to 45 kN. The variance in the capacitance of a single sample depends on the reproducibility of the force imposed under the measurements implied by (1). Analysis of repeated measurements resulted in an error estimation $\delta Q/Q \approx \delta C/C = 0.092$ for single sheets. The data for the individual sheets are contained in table 2 (parts A and B) in the rows labeled $n = 1$. The variation among samples poled under identical conditions is exemplified by results from measurements on samples 34a-d, 36a-d, and 38a-d. The average values and the variation as determined by the standard deviations for these batches are:

Batch 34 C = 14.1 ±1.1 nF, Q/F = 9.7 ±0.9 pC/N;
Batch 36 C = 13.6 ±0.1 nF, Q/F = 9.5 ±0.7 pC/N;
Batch 38 C = 13.7 ±0.0 nF, Q/F = 9.8 ±0.5 pC/N.

In the two parts of table 2 are shown measured values for the capacitance and piezoelectric activity for stacks having n = 1, 2, 4, 6, 8, 9, 10, 14, and 15 sheets. The entries are arranged in chart form to show from which particular sheets each stack or intermediate stage was built. For $n > 2$ there are three sets of entries for each stack or stage: the first set gives the measured values [capacitance (nF) on top, piezoelectric activity (pC/N) on bottom] for the particular stack of n sheets; the second set gives average sheet values, i.e., the first set values divided by n; and the third set gives weighted average values based on the expected contribution of the constituents. That is, the values at the previous stage of each of the constituents were averaged with weighting factor equal to the number of sheets in the constituent stack.

The two intermediate stacks of 15 sheets were assembled into stack 7. One-thirtieth of the measured value of 360 pC/N yields C = 12.0 nF, and Q/F = 12.0 pC/N. The average values for all 30 of the single sheets are C = 13.6 ±0.5 nF and Q/F = 9.8 ±0.7 pC/N. Also, the average of the measured values per layer for the two stacks of 15 sheets is C = 12.9 nF and Q/F = 11.5 pC/N. In this example, the measured value for the piezoelectric activity per layer increases as the stack thickness (proportional to n) increases. An explanation may be that sheets located near the center of the stack undergo greater distortion than sheets near the surface when a given force is applied to the stack.

2.4 Analyses of Piezo-Polymer Electrical Outputs

2.4.1 Summary of Mathematical Development — Appendices A through E are mathematical analyses of the output from a polymer piezoid under various conditions. Appendix A is a circuit analysis of an active polymer element under dynamic loading conditions. This analysis permits calculation of energy and voltage outputs as seen by an R-C load as the piezoid experiences impact. Appendix B contains an evaluation of the formulae for the output due to triangular, half-sine, and haversine force pulses (the haversine pulse has the shape of that of the half sine squared). Appendix C constitutes an analysis of the open-circuit, static-loading voltage and charge levels developed across a piezo-polymer and the subsequent electrical output upon application of an electrical load. Appendix D is a table based on the results developed in appendices B and C and constitutes a summary of polymer piezoid outputs (voltage, energy, charge) under given conditions.

Appendix E is a discussion of the output from a piezoid sample which has non-uniform conductivity and dielectric constant. It was assumed in the analysis given in appendix A that conductivity and dielectric constant are uniform over the sample thickness. It is shown that under practical conditions no modification of the formulae developed in appendices A through C is necessary.

The theoretical conclusions show that to obtain the largest possible transfer of energy stored in the stack, either a series- or parallel-connected stack of n sheets may be constructed, and a switch arrangement should be used with a value of $R_L C$ much smaller than the transfer time (the series stack value of C decreases as n^{-1}). For the dynamic loading arrangement, $R_L C$ should be chosen to satisfy the relation $R_L C \approx \frac{1}{2}\tau$; then in time τ an energy transfer of approximately 40% of the energy stored in the stack, 40% of $Q^2/2C$, will take place. [As a numerical example, consider the values $\tau \approx 10$ μs, $n = 20$, $C \approx 20 \times 12$ nF, and $R_L \approx 20$ Ω. For $Q/F_o \approx 300$ pC/N (2.7 μC/tonf), the maximum output from $F_o = 89$ kN (10 tonsf) would be approximately 0.73×10^{-3} J (7,300 ergs). For the same conditions, but using $R_L = 100$ MΩ, the energy transferred would be reduced by a factor of 0.67×10^{-6}; while if $R_L = 4\Omega$, the energy transferred would be reduced to 0.5 of the maximum value.]

The theory also shows that to obtain the largest output voltage from a stack, the stack should be series connected and the quantity $\nu\tau$ should be $<< 1$ ($\nu\tau$ is defined as the product of the reciprocal of the circuit decay time and the pulse half-width of applied force).

2.4.2 Energy-Release Experiments on Piezo-Polymer Stacks Connected Across an Electrical Load — Described are dynamic and static energy-release experiments on three different multilayered stacks, each with individual component sheets connected in parallel.

2.4.2.1 The voltage output of stack No. 7 was measured across various electrical loads under impact conditions. The stack was mounted on the impact table (a steel cylinder) of a drop-test machine, and the electrical output into a given load was measured and recorded during the impact sequence. A commercially

available accelerometer was attached to the upper face of the dropping carriage and had a specified sensitivity of 7.9 mV/g_n* over the frequency range 5 Hz to 15 kHz. The outputs from stack and accelerometer were stored in a two-channel transient recorder and could be plotted as a function of time on an X-Y_1-Y_2 plotter and displayed on the screen of a monitor storage oscilloscope. A mass of 2.59 kg (corresponding to a weight of 5.69 lb), consisting of an aluminum impactor mounted on the carriage, was released from a height of 5 cm (2 in) to fall freely and impact the polymer stack. The impactor surface was a portion of a sphere with radius 23 cm (9 in). The voltage output from the calibrated accelerometer showed that the maximum force (F_o) developed during impact was 23.8 kN (2.67 tonsf). The resistive load (R_L) was varied between 4 Ω and 40 kΩ. The voltage was measured both with no capacitive load and with a capacitive load (C_L) of 0.5 μF. Actually the transient recorder has an impedance (R_{tr} = 1 MΩ, C_{tr} = 15 pF) which is in parallel with the load; thus the net resistive load was equal to the product of R_L and R_{tr} divided by their sum, and the net capacitive load was equal to the sum of C_L and C_{tr}. The measured data are given in table 3. The energy delivered to the load during the force rise time τ was calculated from the data and is also given in table 3.

Table 3 shows that the voltage maxima and minima for different resistive and capacitive loads behave as predicted by the analysis of appendix B. The output pulse width t_o also agrees with the calculated value. However, the output voltage waveform for large ντ (small R_L) was qualitatively different from that predicted for triangular and half-sine force pulses. For large R_L a square wave would be the likely form expected, with the signal rising in a time much less than τ and then falling to V^{MIN} at τ, with a fast decay time comparable to the rise time. In fact a gradual rise to V_L^{MAX} at the time entered in table 3 was observed. This apparent discrepancy from predicted behavior is the result of the fact that both the triangular and half-sine waveform force pulses have a discontinuity in the time derivative of the force, dF(t)/dt, at t = 0; thus the current $i_G(t)$ would be abruptly turned on at t = 0. Because of the nature of the elastic properties of the polymer, the impacting force is better characterized by a waveform which has both zero derivative and instantaneous value of impacting force at t = 0. After t = 0 both F(t) and $i_G(t)$ should gradually rise from zero value. The voltage and energy integrals for the haversine waveform force pulse (which has these desired properties) have been evaluated in appendix B. There is agreement between the voltage pulse shapes predicted in appendix B, section 3, and those that have been observed during the drop-test evaluations of stack output.

A noticeable difference between the static and dynamic capacity of the test polymer stack was detected in the course of measurements. The capacitance of stack No. 7 was measured statically on the hydraulic press as described in 2.3 (and as also follows from the open-circuit analysis of appendix C) and found to be 0.36 μF. The stack capacitance was then measured at 1 kHz on an impedance bridge with the result of 0.25 μF. According to (31) or (51) of appendix B, the capacitance may also be calculated from the peak voltage data at large R_L given in table 3:

$$\zeta^{-1} = 1 + C_L/C = 22.5/7.5 = 3. \qquad (3)$$

*g_n = 9.81 m/s^2

Since C_L = 0.5 μF, C = (3 - 1)$^{-1}$ x 0.5 μF = 0.25 μF. This result agrees with that of the bridge measurement.

The piezoid may be characterized by its frequency-independent static voltage response to unit force V_o/F_o. For stack No. 7,

$$V_o/F_o = (355\ pC/N)/(0.36\ \mu F) = 1\ mV/N. \quad (4)$$

A comparison value for a typical piezoelectric ceramic (lead zirconium-lead titanate-4) is 0.2 mV/N.

The individual polymer sheets (average capacitance, 13.6 nF; average piezoelectric activity, 9.8 pC/N) also yield this characteristic voltage. Since $V_o/F_o = d_{33}/C_p$, and C_p is proportional to A (30 cm^2 for the piezoid sheets), another quantity that may be used to characterize sheet performance is voltage output in a unit pressure field:

$$V_o A/F_o = 3\ \mu V/Pa. \quad (5)$$

The difference between the effective charge output observed at low and high frequencies (between 0.35 μF x V_o and 0.25 μF x V_o) may be explained by assuming that C is frequency dependent while C_p is not (see appendix B). The dipole orientational contribution to the dielectric constant is frequency dependent according to Debye's theory of polar molecules [4]. The polarizability and relaxation frequency should be much lower for the polarized portion of the piezoid than for the unpoled portion according to the following explanation. The unpoled portion can respond in synchronism to a driving field, while the poled portion of the polymer is saturated. This situation causes the dielectric constant and the resistivity of the poled portion to be less than that of the unpoled portion [5]. The analyses in appendices A through C were carried out under the assumption that the dielectric constant and resistivity were homogeneous throughout the piezoid. In appendix E it is shown that under practical conditions even when the dielectric constant and resistivity vary through the material, the formulas are still valid.

The data in table 3 may be interpreted in terms of the haversine force pulse analysis presented in appendix B, and comparisons made between measured and theoretically predicted values. Consider as examples: { 1 } the time t_M at which $V_L = V_L^{MAX}$ and the duration t_o of V_L regarded as a pulse, { 2 } the behavior of the maximum and minimum (positive and negative) voltage peaks of V_L, and { 3 } the relationship between the energy *E* delivered to the load and the load resistance R_L.

In example { 1 }, for large values of R_L (corresponding to small values of the product $\nu\tau$), the theory predicts that the time at which V_L reaches maximum value is equal to the rise time τ of the force pulse and that t_o equals 2τ. The measured values for R_L = 40 kΩ confirm this prediction; that is, twice the time (measured from 0) at which V_L is maximum equals t_o (2 x 225 = 450). For small values of R_L (corresponding to large values of $\nu\tau$), the theory predicts that t_o should be approximately equal to τ with the V_L

maximum occurring at $\tau/2$. Again, the measured values for $R_L = 4\ \Omega$ confirm this prediction, with $t_o = \tau = 225$, although the agreement is not as good for the time at which V_L^{MAX} occurs (2 x 100 is only approximately equal to 225).

In example { 2 }, the relative magnitudes of the positive and negative voltage peaks V_L^{MAX} and V_L^{MIN} agree with theoretical prediction: for large values of R_L, the measured values of V_L^{MIN} tend toward zero [see (62)], and V_L^{MAX} depends on the value of C_L as given in (63) [see also (23)]. For small values of R_L, the theory (60) predicts that $V_L^{MIN} = -V_L^{MAX}$, and the measured values agree for R_L as large as 40 Ω. Further, theory predicts that the peak values exhibit no dependence on C_L for small values of R_L; comparison of the measured values of V_L^{MAX} given in table 3 for two values of C_L confirms this independence (0.14 ≈ 0.15; 0.40 = 0.40).

In example { 3 }, the theory predicts (65) that the value of $\nu\tau$ for maximum energy transfer into the load should be approximately equal to $\tau/R_LC + 2.1$. R_L therefore would be predicted to be $\frac{225}{(0.25)(2.1)} = 430\ \Omega$, which is in reasonable agreement with the measured value of 400 Ω. The normalized value, for maximum energy transferred into the load, $E(\tau)/F_o^2$, was computed from measurements to be 61.6 femtojoules per newton squared (fJ/N^2), which agrees well with the theoretically predicted value of 59 fJ/N^2. This value and other calculated values given in table 4 were calculated from equations derived in the haversine force pulse analysis (and also summarized in appendix D, condition 3):

$$\left.\begin{aligned} (V_L/F_o)^{MAX} &\approx \frac{\pi R_L C}{2\tau}\,\frac{V_o}{F_o} = 1.724\ R_L\ (\mu V/N) \\ E(\tau)/F_o^2 &\approx \frac{R_L}{8\tau}\,\left(\frac{\pi C V_o}{F_o}\right)^2 = 0.334\ R_L\ (fJ/N^2) \end{aligned}\right\} \quad \nu\tau \gg 1,$$

$$\left.\begin{aligned} (V_L/F_o)^{MAX} &\approx \zeta\ V_o/F_o = 1000\ \zeta\ (\mu V/N) \\ E(\tau)/F_o^2 &\approx \frac{3\tau}{8R_L}\,\left(\frac{\zeta V_o}{F_o}\right)^2 = \frac{84.4}{R_L(k\Omega)}\ (fJ/N^2) \end{aligned}\right\} \quad \nu\tau \ll 1. \qquad (6)$$

Comparison of the measured and calculated values of the various parameters given in table 4 shows good agreement between the experimental results and theoretical prediction.*

---

*From the general expression for V_L, (56), V_L^{MAX} was calculated to occur at $t = 0.78\tau = 175\ \mu s$, and V_L^{MAX}/F_o was calculated to have the value $(V_o/2F_o)$ x (0.831) x (1.156) = 480 μV/N.

2.4.2.2 By means of mechanically charging an initially open-circuited piezoid which subsequently had its energy released when a preset stack voltage was reached, a pyrotechnic actuator (the electrical load) supplied by the sponsor was fired.

In order to test the predictions of appendix C, the circuit shown in figure 4 was designed to establish an open-circuit condition across the polymer stack. When the voltage resulting from a force applied to the piezoid rises to a predetermined level (the value used was 20 V), the Zener diode triggers the gate of the SCR, which in turn permits the energy stored in the polymer device to flow into the load. The load selected was a pyrotechnic actuator which on receiving 800 ergs (8×10^{-5} J) changed its dc resistance from 3 Ω to 2 kΩ and its capacitance from 1 μF to 1 nF. The values given are approximate.

Stack No. 5 was used for this test with successful results. It was found that a force of 73 kN (8.2 tonsf) triggered the circuit and produced a signal of 23 V with the load being the input circuit of an oscilloscope (input impedance 1 MΩ, shunted by 18 pF. Stack No. 5 (88 sheets; see table 5) had a measured static output of 290 pC/N with a static capacitance of 1 μF. The static voltage level was calculated according to (4) to be $V_o/F_o = 0.29$ mV/N. The expected voltage level for the force (applied with the hydraulic press) was $V_o = 21$ V. For these parameters ($\zeta^{-1} = 2$ and $\nu^{-1} \approx \zeta^{-1} R_L C \approx 6 \times 10^{-6}$), the energy output to the actuator was calculated using (56) and (58) to be 1100 ergs delivered at approximately 10 V.

Note that if the actuator had been connected directly across the piezoid, a force of 73 kN with a rise time of $\tau = 10$ μs* would have yielded $V_L(\tau) \approx 6$ V and $E(\tau) = 418$ ergs. At 6 V, the threshold energy for the actuator is 1000 ergs; direct coupling therefore would not provide sufficient energy to the load.

2.4.2.3 An impact test was carried out at the air-gun installation in the Harry Diamond Laboratory in which a stack was directly impacted by a high-velocity projectile. A flat-nosed projectile with a mass of 1.38 kg was fired from a gun with a bore of 10 cm (4 in) at a polymer piezoid made from 20 sheets. The velocity at impact was determined to be 154 m/s (504 ft/s). The force sustained by the polymer stack was estimated by the air-gun test personnel on the basis of experience to be 450 kN (50 tonsf). A high-resistance probe ($R_L = 100$ MΩ, $C_L = 3$ pF) was placed across the sample, and voltage output was recorded photographically from calibrated oscilloscopes which were triggered by means of a trip wire 40 μs before impact. Following impact, the recorded voltage rose linearly to a peak of 200 V at 0.48 μs after impact. According to calculation on the basis of the formulas given in appendix B, the voltage produced should be 400 V.† During the initial impact

---

*$\nu\tau = 1.67$; $\beta(1.67) = 0.379 \approx 0.381$, its maximum value; see appendix B.

†$\tau/R_L C = 0.48$ μs/(100 MΩ) (0.26 μF) $= 1.8 \times 10^{-8}$, which is much less than one; $V_L(\tau) = Q_o/C = (233$ pC/N) $(4.5 \times 10^5$ N)/0.26 μF = 400 V.

duration of 0.48 μs, the energy delivered to the load was only 64 pJ because of the extreme mismatch of the 100 MΩ load. Note that if R_L had been chosen as 4 Ω, then instead of 200 V, a voltage peak of 160 V and an energy output of 1.15 mJ would have been expected; while if R_L had been chosen to optimize the energy output ($R_L \approx 1\ \Omega$), a voltage peak of 90 V and $E^{MAX}(\tau) = 1.98$ mJ would have resulted.

3. DELIVERIES

A tabulation of the PVF_2 piezopolymer stacks which were delivered to Frankford Arsenal is given in table 5. The entries in the column labelled "Total Activity" were measured with an estimated sample single standard deviation of ±10% by the static open-circuit test method described in 2.3. The final column gives the average activity per sheet, the quotient of the values in the "Total Activity" column and the number of sheets in the given stack.

In all cases, the individually poled PVF_2 sheets had congruent 30-cm^2 circular aluminum electrodes vacuum deposited on both sides of the sheet. The thickness of each stack is made up of contributions from n polymer sheets, $2n$ electrodes, and n - 1 bonds. The nominal poling conditions for stack Nos. 1-6 were 95°C for the maximum temperature and 1200 V for the poling potential; to achieve more effective poling, the nominal poling conditions for stack Nos. 7-10 were 120°C for the maximum temperature and 2000 V for the poling potential.

4. SUMMARY AND RECOMMENDATIONS

4.1 Summary

A piezoelectric polymer transducer, with an active element of area 30 cm^2 and thickness less than 0.9 mm, has been developed that is capable of delivering into a several-ohm load an energy of 0.32 mJ in response to a 89-kN impact having a rise time of 10 μs.* In support of this development, specific poling methods and methods of stack construction were evolved.

Static and dynamic test methods have been developed to characterize the electrical output and piezoelectric activity of polymer elements, or piezoids. The static method makes use of an hydraulic press to apply force to the piezoid; in the dynamic method, the piezoid is impacted with a known force in a drop-test machine.

Theoretical analyses, in particular applying to both test-method situations, have been formulated to predict the electrical output of a stack under various conditions. The theoretical predictions are in good agreement with the experimental measurements that have been made, especially for the haversine-force pulse model of the drop-test situation.

---

*The values cited refer to Stack No. 7, which was slightly thicker than the 0.7-mm value specified. Stack No. 8 met all the requirements given in 1.2, with a thickness of 0.68 mm and an output under the specified conditions and into the specified load of 0.24 mJ.

4.2 Recommendations

Theoretical [6] and experimental studies [7] in our laboratory and elsewhere indicate that most of the activity of a polymer film occurs in very thin layers near each electrode and that the bulk of the material is relatively inert. A conclusion that requires further experimental verification is that higher activity should be achieved with the use of thinner sheets, since less "inert" material would be present. The activity of two 9-μm PVF_2 samples was measured in our laboratory and found to be approximately twice that of two 30-μm samples said to be poled with the same field strength according to the supplier. If more empirical evidence becomes available supporting the use of thin polymer sheets or films to achieve high piezoelectric activities, techniques of depositing very thin polymer films on suitable substrate material should be considered.

Other means of improving per-sheet activity, for example, multiple poling cycles, the use of high-frequency electrical poling pulses, and treatment such as stretching prior to electrical poling, require investigation.

The methods of test need to be further developed to improve the precision of results. The use of a commercially available force transducer for calibration is recommended.

Results of measurements on completed stacks show that the activity of the stack as a whole tends to be greater than the sum of the activities of the individual sheets. This phenomenon should be investigated, as it may hold clues to improved stack design leading to higher per-stack activities.

APPENDIX A

Output from Piezoid Sample Under Dynamic Loading Conditions

Voltage and charge measurements have been conducted during static- and dynamic-loading experiments on single polymer sheets and on stacks of active and inactive polymer sheets electrically connected in both series and parallel.

Consideration of the results of these tests has led to the equivalent circuit shown in figure 2. The polymer is modeled as consisting of two uniform parts: An active part in series with an inactive region. The active part is understood to coincide with the poled portion, is denoted by the letter "P", and has a thickness ℓ_P. The inactive, unpoled portion may be regarded as a shunt with respect to P, is denoted by the letter "S", and has a thickness ℓ_S. Each part is modeled separately as a parallel R-C circuit with a charge Q on C and a current i in R. Theoretical and experimental results for a poled sample show that the surface regions are strongly poled, while the bulk of the interior is less effectively poled. Figure 3 shows the polymer element with a series load of resistance R_L (with current i_L) and capacitance C_L (with charge Q_L).

Consider a piezoelectric material. A pair of equivalent piezoelectric equations relate electric field E, electric displacement D, and stress T.[8]

$$E_n = \beta^T_{nm} D_n - g_{nm} T_m \tag{7}$$

and

$$D_n = \varepsilon^T_{nm} E_m + d_{nm} T_m, \tag{8}$$

expressed in Einstein summation convention.

In this convention, β is the dielectric impermeability tensor (elements β_{nm}), and g is the piezoelectric stress tensor (elements g_{nm}), which are related to the dielectric permittivity ε and the piezoelectric strain d, respectively by:

$$\beta = \varepsilon^{-1} \quad \text{and} \quad g = \varepsilon^{-1} d\,. \tag{9}$$

If stress T is applied uniformly to the piezoid (in a direction perpendicular to the plane of the polymer (i.e., in the negative-3 direction), a voltage V develops across its thickness ℓ and charge Q appears at the surface of area A. It is assumed that in a polymer the polarization is induced predominantly parallel or antiparallel to the poling field direction. After poling when a stress in any direction is applied to the poled material, the voltage along directions other than the poling direction are negligible. This implies that the dielectric tensor elements ε_{3i}, ε_{i3}, β_{3i}, β_{i3} are zero when $i \neq 3$, and that the g_{nm} and d_{nm} tensors have non-zero elements only in the row n = the poling direction.

Note that

$$C_P = \varepsilon_P A/\ell_P \quad C_S = \varepsilon_S A/\ell_S, \; C^{-1} = C_P^{-1} + C_S^{-1}, \text{ and } Q = CV. \tag{10}$$

Integration of (7) under the conditions D = 0 inside the piezoid (the open circuit condition), g ≠ 0 only across the poled portion, and the applied force F = AT, yields:

$$V = -\int_0^{\ell} E dx_3 = \frac{\ell_P}{A} gF = \frac{d_{33}}{C_P} F \text{ and } Q = \frac{C}{C_P} d_{33} F. \tag{11}$$

The quantity d_{33} is taken as the longitudinal piezoelectric constant of a poled polymer.

For short-circuit conditions, E is zero inside the piezoid, and it is convenient to use equation (8). As a stress is imposed, a short-circuit current equal to the displacement current is generated in the piezoid. This current is:

$$i = A \frac{dD}{dt} = d_{33} \frac{dF}{dt} \equiv d_{33} \dot{F}. \tag{12}$$

The sign of the force for compression is opposite to that for tension, and the sign of the resulting charge is also opposite for compression to that for tension.

During the application of a time-dependent force to the polymer, the active portion of the piezoid (see figures 5 and 6) acts as a generator of current i_G. As a convention,

$$i_G(t) = d_{33} \dot{F}(t). \tag{13}$$

The current, i = i(t), flowing in the external circuit is predominantly determined by the electrical load. Under dynamic loading [$C_L \neq 0$, $R_L \neq \infty$], some of the generated power is lost internally to R_P and R_S.

Application of Kirchoff's laws to the circuits in figures 5 and 6 yields:

$$i_L R_L + i_P R_P + i_S R_S = 0, \tag{14}$$

$$i = i_G + i_P + \dot{Q}_P = i_S + Q_S = i_L + \dot{Q}_L, \text{ and} \tag{15}$$

$$0 = i_L R_L - Q_L C_L^{-1} = i_S R_S - Q_S C_S^{-1} = i_P R_P - Q_P C_P^{-1}. \tag{16}$$

Substituting in (14) and (15) for i_P, i_S, and i_L in terms of Q_P, Q_S, and Q_L as given in (16 yields:

$$Q_L C_L^{-1} + Q_P C_P^{-1} + Q_S C_S^{-1} = 0, \tag{17}$$

$$\dot{Q}_S + (R_S C_S)^{-1} Q_S = \dot{Q}_L + (R_L C_L)^{-1} Q_L, \text{ and} \tag{18}$$

$$\dot{Q}_P + (R_P C_P)^{-1} Q_P = \dot{Q}_L + (R_L C_L)^{-1} Q_L - i_G. \tag{19}$$

The time derivative of (17) added to the product of (17) and the quantity $(R_pC_p)^{-1}$ give:

$$0 = C_L^{-1}[\dot{Q}_L + (R_pC_p)^{-1}Q_L] + C_p^{-1}[\dot{Q}_p + (R_pC_p)^{-1}Q_S]. \tag{20}$$

In solving (20), (18), and (19) it is convenient to assume that

$$R_pC_p = R_SC_S.* \tag{21}$$

This relation holds if the active and inactive portions have the same conductivity and dielectric constant, since C and R are inversely and directly proportional to thickness, respectively. Substituting first (19) into (20) and then (18) with $(R_SC_S)^{-1}$ replaced by $(R_pC_p)^{-1}$ into (20) gives the result:

$$\dot{Q}_L + \nu Q_L = \zeta \frac{C_L}{C_p} i_G, \tag{22}$$

where

$$\nu = \zeta\left(\frac{1}{R_LC} + \frac{1}{R_pC_p}\right),\ \zeta = \left(1 + \frac{C_L}{C}\right)^{-1},\ \text{and}\ C^{-1} = C_p^{-1} + C_S^{-1}. \tag{23}$$

The solution of (22) is given by

$$Q_L(t) = \zeta\frac{C_L}{C_p}\int_0^t dt' \exp(\nu t' - \nu t) i_G(t'). \tag{24}$$

From (16) and (13),

$$i_L(t) = (R_LC_L)^{-1}Q_L(t) = (R_LC_p)^{-1}\zeta d_{33}\int_0^t dt' \exp(\nu t' - \nu t)\dot{F}(t'). \tag{25}$$

The voltage across the load is

$$V_L(t) = R_L i_L(t), \tag{26}$$

while the energy delivered thereto is given by

$$E(t) = \int_0^t dt' R_L i_L^2(t'). \tag{27}$$

For stacks consisting of n piezoid sheets electrically connected in series or parallel (k indicates kth sheet]:

$$0 = i_LR_L - Q_LC_L^{-1} = i_{S_k}R_{S_k} - Q_{S_k}C_{S_k}^{-1} = i_{P_k}R_{P_k} - Q_{P_k}C_{P_k}^{-1}. \tag{28}$$

For the parallel arrangement,

$$i_LR_L + i_{P_k}R_{P_k} + i_{S_k}R_{S_k} = 0, \text{ and} \tag{29}$$

*See appendix E.

$$i = i_L + \dot{Q}_L = \sum_{k=1}^{n} i_k, \tag{30}$$

where

$$i_k = i_{G_k} + i_{P_k} + \dot{Q}_{P_k} = i_{S_k} + \dot{Q}_{S_k}.$$

For the series arrangement,

$$i_L R_L + \sum_{k=1}^{n} (i_{P_k} R_{P_k} + i_{S_k} R_{S_k}) = 0, \text{ and} \tag{31}$$

$$i = i_L + \dot{Q}_L = i_{G_k} + i_{P_k} + \dot{Q}_{P_k} = i_{S_k} = \dot{Q}_{S_k}. \tag{32}$$

If the sheets have identical electrical characteristics, the subscript k may be dropped and the summations may be replaced by a multiplicative factor, n.

Then for the parallel case,

$$(1 + \frac{C_L}{nC})\ \dot{Q}_L + (\frac{1}{nR_L C} + \frac{1}{R_P C_P})\ Q_L = \frac{C_L}{C_P}\ i_G, \tag{33}$$

For the series case,

$$(1 + \frac{nC_L}{C})\ \dot{Q}_L + (\frac{n}{R_L C} + \frac{1}{R_P C_P})\ Q_L = \frac{C_L}{C_P}\ n i_G\ . \tag{34}$$

Thus in (23) through (27) all symbols remain the same except that for the parallel case

$$C \rightarrow nC, \tag{35}$$

while for the series case

$$C \rightarrow n^{-1}C \text{ and } i_G \rightarrow n i_G. \tag{36}$$

Note that the polymer resistance term occurs only in the combination $R_P C_P$ and that the value of this product does not change whether the arrangement is series or parallel.

APPENDIX B

Evaluation of the Output for Triangular-, Half-Sine- and Haversine-Waveform Force Pulses

1. Triangular Force Pulse

The triangular force pulse is characterized by:

$$F(t) = \begin{cases} (t/\tau)F_o, & 0 \le t \le \tau \\ (2 - t/\tau)\, F_o, & \tau \le t \le 2\tau \end{cases} . \tag{37}$$

Then

$$V_L(t) = \zeta V_o(\nu\tau)^{-1} \begin{cases} (1 - e^{-\nu t}), & 0 \le t \le \tau \\ (2e^{\nu\tau} - 1 - e^{\nu t})e^{-\nu t}, & \tau \le t \le 2\tau. \\ -(e^{\nu\tau} - 1)^2\, e^{-\nu t}, & 2\tau \le t \end{cases} \tag{38}$$

Also

$$E(\infty) = E_o \delta(\nu\tau),\ E_o = \zeta C V_o^2 (1 + \frac{R_L C}{R_P C_P})^{-1}, \tag{39}$$

where

$$\delta(Y) = \frac{2}{Y} - \frac{1}{Y^2}\,(3 - e^{-Y})(1 - e^{-Y}),\ Y = \nu\tau, \text{ and } V_o = \frac{d_{33}F_o}{C_P} . \tag{40}$$

Since R_P is greater than $10^{12}\Omega$, $R_L << R_P$; consequently, $\nu^{-1} \simeq R_L(C + C_L)$, and $E(\infty) = (C + C_L)^{-1}Q_o^2\, \delta(Y)$ where

$$Y \approx \frac{\tau}{R_L(C + C_L)} \text{ and } Q_o = \frac{C d_{33} F_o}{C_P} = CV_o. \tag{41}$$

The voltage has its maximum at time $t = \tau$, where $V_L(\tau) = Y^{-1}(1 - e^{-Y})\zeta V_o$; this expression is a monotonic decreasing function of Y. Then,

$$V_L(\tau) \simeq \begin{cases} \dfrac{Q_o}{C + C_L} = \zeta V_o, & Y << 1 \\ \dfrac{R_L Q_o}{\tau} = \dfrac{R_L C}{\tau} V_o, & Y >> 1 \end{cases} . \tag{42}$$

The minimum value of the voltage occurs at time $t = 2\tau$ where $V_L(2\tau) = -(1 - e^{-Y})V_L(\tau)$. This expression has its least values for Y small and large,

$$V_L(2\tau) \approx \begin{cases} -YV_L(\tau), & Y \ll 1 \\ -V_L(\tau), & Y \gg 1 \end{cases}, \tag{43}$$

and its largest value at $Y \approx 1.2565$, where

$$V_L(2\tau) = \frac{-0.407\ Q_o}{C + C_L} = -0.407\zeta V_o = -0.715\ V_L(\tau).$$

The voltage has value zero for t_o given by

$$t_o = \nu^{-1}\, \ell n(2e^Y - 1),\ \tau \le t_o \le 2\tau;$$
$$t_o \gtrsim \tau,\ Y \gg 1; \quad t_o \lesssim 2\tau,\ Y \ll 1. \tag{44}$$

The energy has a maximum when the load resistance is chosen to be an appropriate value for a given rise time and polymer capacitance. That is, $\delta(Y)$ reaches its maximum 0.381 at $Y = 1.893$. Then

$$E_{(\infty)}^{MAX} = \frac{0.381\ Q_o^2}{C + C_L} = 0.381\zeta C V_o^2. \tag{45}$$

Note that $\delta(Y = 0.25) = 0.139$; $\delta(Y \le 0.25) \approx \frac{2}{3} Y - \frac{1}{2} Y^2$; $\delta(Y = 4) = 0.317$; and $\delta(Y \ge 4) \approx \frac{2}{Y} - \frac{3}{Y^2}$. When $Y \gg 1$ (very small R_L),

$$E(\infty) \approx \frac{2R_L}{\tau}\ Q_o^2. \tag{46}$$

Calculation of the energy delivered to the load during time $t = \tau$ and $t = 2\tau$ yields

$$E(\tau) = \frac{1}{2} E(\infty) \text{ and } E(2\tau) = E_o \delta_2(\nu\tau), \tag{47}$$

where

$$\delta_2(Y) = \delta(Y) - \frac{1}{2Y^2}(1 - e^{-Y})^4.$$

For the values $\tau = 10^{-5}$s, $R_L = 4\Omega$, and $C = 0.3\ \mu F$, $Y \approx 8$ and the approximation of (46) is valid. With the expression of (41) or (70) for the effective charge Q_o developed on the capacitor, (46) and (47) yield $E(\tau) \approx R_L Q_o^2/\tau$.

Under optimum conditions, as given in (45), E^{MAX} increases linearly with the number of sheets in a stack, n, whether the sheets are connected in series or parallel. For $Y \gg 1$, the energy is independent of n for series connection; for parallel connection, the energy varies as n^2. However for $Y \ll 1$ (i.e., very large R_L),

$$E(\infty) = \frac{2\tau}{3R_L} \frac{Q_o^2}{(C + C_L)^2} = \frac{2\tau}{3R_L} (\zeta V_o)^2, \tag{48}$$

and the remarks applying to series and parallel stacks are reversed.

2. Half-Sine Force Pulse

For the half-sine pulse given by

$$F(t) = F_o \sin \frac{\pi t}{2\tau}, \quad 0 \le t \le 2\tau, \tag{49}$$

$$V_L(t) = \zeta V_o \cos\phi \begin{cases} \sin(\frac{\pi t}{2\tau} + \phi) - e^{-\nu t} \sin\phi, & 0 \le t \le 2\tau \\ -(1 + e^{2\nu\tau})\, e^{-\nu t} \sin\phi, & 2\tau \le t \end{cases} \tag{50}$$

where

$$\tan\phi = \frac{2}{\pi} \nu\tau. \tag{51}$$

For continuous sinusoidal force the first equation of (50) applies with $0 \le t < \infty$.

Note that if $\nu\tau \ll 1$, the voltage reaches its maximum at $t = \tau$. Then

$$V_L(\tau) \approx \zeta V_o \tag{52}$$

and the minimum occurs at $t = 2\tau$, where

$$V_L(2\tau) \approx - \frac{4Y}{\pi} V_L(\tau). \tag{53}$$

(As a numerical example, consider the following: a frequency of 100 Hz corresponds to $\tau = 2.5$ ms; a stack of $n = 4$ sheets in series corresponds to a value of $C \approx 0.0025$ μF; for $R_L = 10$ MΩ, $\nu\tau \approx \tau/R_L C \approx 0.10$.)

If in addition $C_L \ll C$ and if the stack is made up of sheets connected electrically in parallel, $V_L(\tau)$ is unaffected, while $V_L(2\tau)$ depends on n^{-1}; but for the series connection, $V_L(\tau)$ varies as n, and $V_L(2\tau)$ depends on n^2.

On the other hand, if $\nu\tau >> 1$, the voltage amplitude is reduced considerably. The voltage minimum occurs at $t = 2\tau$, and the voltage maximum occurs at t on the order of $\nu^{-1} \approx R_L C << \tau$, since $\phi \approx \frac{\pi}{2} - \frac{\pi}{2\nu\tau}$:

$$V_L^{MAX} \approx \frac{\pi R_L C}{2\tau} V_o \approx -V_L(2\tau). \tag{54}$$

(As a numerical example, consider the following: a frequency of 1 kHz corresponds to $\tau = 0.25$ ms; a stack of $n = 4$ sheets in parallel corresponds to a value of $C \approx 0.40$ μF; for $R_L = 100\ \Omega$, $\nu\tau \approx \tau/R_L C = 57$.)

If a stack consists of n sheets electrically in parallel, V_L^{MAX} is increased n-fold times; for the series connection, V_L^{MAX} is unaffected.

3. Evaluation of the Output for Haversine Waveform Force Pulse

For the haversine pulse given by

$$F(t) = \frac{1}{2} F_o \left(1 - \cos \frac{\pi t}{\tau}\right) = F_o \sin^2 \frac{\pi t}{\tau},\ 0 \le t \le 2\tau, \tag{55}$$

$$V_L(t) = \frac{1}{2} \zeta V_o \sin\theta \begin{cases} \sin\left(\frac{\pi t}{\tau} - \theta\right) + e^{-\nu t} \sin\theta,\ 0 \le t \le 2\tau \\ -(e^{2\nu\tau} - 1)\, e^{-\nu t} \sin\theta,\ 2\tau \le t \end{cases} \tag{56}$$

where [see (51)]

$$\cot\theta = \frac{\nu\tau}{\pi} = \frac{1}{2} \tan\phi. \tag{57}$$

The energy is calculated as

$$E(\infty) = 2E(\tau) = \frac{1}{4} E_o g(\nu\tau,\ \nu\tau/\pi)$$

$$E(2\tau) = \frac{1}{8} E_o g(2\nu\tau,\ \nu\tau/\pi) \tag{58}$$

where

$$g(a,b) = (1 + b^2)^{-1} \left[a + (1 + b^2)^{-1}(1 - e^{-2a})\right]. \tag{59}$$

Here for $\nu\tau >> 1$ the voltage rises slowly to a maximum at $t = \frac{1}{2}\tau$, falls gradually to zero at $t = \tau$, and then reaches a minimum at $t = \frac{3\tau}{2}$. Then since $R_L/Rp << 1$,

$$V_L^{MAX} \approx \frac{\pi R_L C}{2\tau} V_o \approx -V_L^{MIN}. \tag{60}$$

This behavior contrasts with that of the two force pulses discussed previously. For example, compare this temporal behavior to that described by (38) and (50) for which the voltage rises very quickly in times on the order of $\nu^{-1} \ll \tau$ [see also (43)].

Returning to the haversine pulse, when $\nu\tau \gg 1$ (very small R_L),

$$E(2\tau) \approx E(\infty) \approx \frac{R_L}{4\tau} (\pi Q_o)^2. \tag{61}$$

On the other hand, for $\nu\tau \ll 1$, the voltage behaves as in the previous cases, the maximum occurring at $t \approx \tau$ where

$$V_L^{MAX} \approx \zeta V_o \tag{62}$$

and the zero occurs almost simultaneously with the minimum at $t = 2\tau$ where

$$V_L^{MIN} \approx -\nu\tau\zeta V_o \approx 0. \tag{63}$$

Also if $\nu\tau \ll 1$ (very large R_L),

$$E(2\tau) \approx E(\infty) \approx \frac{3\tau}{4R_L} \frac{Q_o^2}{(C + C_L)^2} = \frac{3\tau}{4R_L} (\zeta V_o)^2. \tag{64}$$

Now the energy, $E(\infty)$ is largest when $\nu\tau$ is chosen so as to maximize the function $g(\nu\tau, \nu\tau/\pi)$. This occurs at $\nu\tau = 2.106$ when $g = 1.922$. Then (with $R_L/R_p \approx 0$)

$$E^{MAX}(\infty) = 0.481 \frac{Q_o^2}{C + C_L} = 0.481\zeta C V_o^2. \tag{65}$$

Because of the close identification between (42) through (48), (52) through (54), and (60) through (65), the remarks in sections 2 and 3 herein about series- and parallel-electrically connected stacks apply to all three pulse waveforms. Note that the inequalities (44) satisfied by t_o, the instant when the voltage null occurs for the triangular pulse, apply also for the half-sine and haversine pulses. Also, it can be proved in general that if the force pulse is symmetric about τ [i.e., if $F(t) = F(2\tau - t)$, $0 \le t \le 2\tau$ and $F(t) = 0$ for all other t], then the identity $E(\infty) = 2E(\tau)$ holds.

APPENDIX C

Piezoid Output Produced by Open-Circuit Charging Followed by Application of an Electrical Load

The polymer stack may be electrically charged under open-circuit conditions by applying pressure with an hydraulic press or by impacting the stack with a moving mass. The developed charge and energy may then be dumped into a load by means of a switch. This procedure results in an optimal charge and energy transfer from the polymer piezoid to the load. The process of charging under open-switch conditions followed by switching in a load is equivalent to turning on a force infinitely rapidly under closed-circuit conditions. This process may be described by the relation

$$F(t) = \lim_{\mu \to \infty} (1 - e^{-\mu t})F_0, \quad t \geq 0. \tag{66}$$

If at $t = 0^+$, i.e., at a time instantaneously greater than $t = 0$, the switch across the load is closed (after application of pressure or after impact), then the voltage level across the load is

$$V_L(t) = \zeta V_0 e^{-\nu t}, \tag{67}$$

the charge which flows off the polymer is given from (15), (22), and (25) of appendix B by

$$Q(t) = \int_0^t dt' i(t') = Q_0\left(1 + \frac{R_L C}{R_P C_P}\right)^{-1}\left[1 - \zeta\left(1 - \frac{R_L C_L}{R_P C_P}\right)e^{-\nu t}\right], \tag{68}$$

and the energy delivered to the load is

$$E(t) = \frac{1}{2}(1 - e^{-2\nu t})E_0 \tag{69}$$

For times long compared to $\nu^{-1} \approx R_L C$, and using the usual approximations ($C_L \ll C$, $R_L \ll R_P$),

$$Q \approx Q_0, \quad E \approx \frac{1}{2} C V_0^2 = \frac{Q_0^2}{2C}. \tag{70}$$

This Q is the charge built up on the polymer stack. Q is independent of n for series electrical connection and proportional to n for parallel connection. The quantity E is the energy stored in the stack and is proportional to n for both series and parallel connections. For times of the order of tens of microseconds and capacitances of the order of tenths of microfarads, R_L should be somewhat less than 100 Ω to have full energy transfer to the load.

However, if R_L is large (certainly if $R_L > 10$ kΩ, and $t < 1.0$ ms),

$$Q(t) \approx \zeta C_L V_o + \frac{\zeta^2 t}{R_L} V_o \text{ and } E(t) \approx \frac{t}{R_L} (\zeta V_o)^2. \tag{71}$$

Note that if $C_L/C < \nu\tau < 1$, the second term in the expression for $Q(t)$ in (71) dominates; however if $C_L/C > \nu\tau$, the first term is larger than the second. If $C_L/C \ll 1$, Q and E are independent of n for the parallel electrical connection, while for the series electrical connection, Q is proportional to n, and E is proportional to n^2.

APPENDIX D

Expressions for Piezoid Output Into Load

	Condition 1			Condition 2			Condition 3			Condition 4	
	Voltage		Energy	Voltage		Energy	Voltage		Energy	Charge	Energy
	V_L^{MAX}	V_L^{MIN}	$E(\tau)$	V_L^{MAX}	V_L^{MIN}	$E(\tau)$	V_L^{MAX}	V_L^{MIN}	$E(\tau)$	$Q(\tau)$	$E(\tau)$
$\nu\tau \ll 1$	ζV_o	$-\nu\tau\zeta V_o$	$\frac{\tau}{3R_L}(\zeta V_o)^2$	ζV_o	$-\frac{4}{\pi}\nu\tau V_o$	$\frac{\tau}{2R_L}(\zeta V_o)^2$	ζV_o	$-\nu\tau\zeta V_o$	$\frac{3\tau}{8R_L}(\zeta V_o)^2$	$\zeta C_L V_o + \zeta^2 \tau V_o / R_L$	$\frac{\tau}{R_L}(\zeta V_o)^2$
$\nu\tau \gg 1$	$\tau^{-1} R_L Q_o$	$-\tau^{-1} R_L Q_o$	$\tau^{-1} R_L Q_o^2$	$(2\nu\tau)^{-1}\pi V_o$	$-(2\nu\tau)^{-1}\pi V_o$	$\frac{\pi^2}{8\tau} R_L Q_o^2$	$(2\nu\tau)^{-1}\pi V_o$	$-(2\nu\tau)^{-1}\pi V_o$	$\frac{\pi^2}{8\tau} R_L Q_o^2$	Q_o	$\frac{1}{2}\zeta C V_o^2$
$(\nu\tau)^*$	$0.449\zeta V_o$	$-0.381\zeta V_o$	$0.190\zeta V_o^2$	$0.483\zeta V_o$	$-0.513\zeta V_o$	$0.263\zeta C V_o^2$	$0.480\zeta V_o$	$-0.408\zeta V_o$	$0.240\zeta C V_o^2$	Q_o	$\frac{1}{2} C V_o^2$

Conditions:

1. When stack is subjected to triangular force pulse; $(\nu\tau)^* = 1.89$ yields maximum.
2. When stack is subjected to half-sine force pulse; $(\nu\tau)^* = 1.73$ yields maximum.
3. When stack is subjected to haversine pulse; $(\nu\tau)^* = 2.11$ yields maximum.
4. After open-circuit storage of charge an electrical load is switched in at $\tau = 0$; when $(\nu\tau)^* \gg 1$, $C_L = 0$ yields maximum.

APPENDIX E

Output from Piezoid Sample Having Non-Uniform Conductivity and Dielectric Constant

Both theoretical and experimental investigations show that the dielectric constant and conductivity of the poled portion of a piezoelectric material are different from the unpoled bulk portion.

In appendix A, the condition $R_S C_S = R_P C_P$, was assumed for convenience of exposition. However, an equation for Q_L can be found by substituting for $\dot{Q} + (R_P C_P)^{-1} Q_P$ from (19) into (17). Then the resulting equation may be combined with (18) to determine an expression for Q_S in terms of $Q_L, \dot{Q}_L$, and i_G. Finally this expression and its time derivative (the expression for Q_S in terms of $\dot{Q}_L$, $\ddot{Q}_L$, and di_G/dt) may be substituted in (18) and there results:

$$[C^{-1} + C_L^{-1}]\,\ddot{Q}_L + [C^{-1}(R_L C_L)^{-1} + (C_L^{-1} + C_S^{-1})\,(R_P C_P)^{-1} + (C_L^{-1} + C_P^{-1})\,(R_S C_S)^{-1}]\,\dot{Q}_L + [(R_P R_L)^{-1} + (R_S R_L)^{-1} + (R_P R_S)^{-1}] \times (C_P C_S C_L)^{-1}\, Q_L = C_P^{-1}[di_G/dt + (R_P C_P)^{-1}\, i_G]. \tag{72}$$

This equation is easily solved; however the solution is lengthly, and therefore only the expression for $R_L \ll R_P$ and R_S, which holds in all practical situations, is given here.

$$i_L = (R_L C_L)^{-1}\, Q_L = \int_0^t dt' i_G(t') \{(R_L C_P)^{-1}\, \zeta \exp[\zeta (R_L C)^{-1}\,(t' - t)] + + (C_P C)^{-1}\,[(R_P C_P)^{-1} - (R_S C_S)^{-1}] \exp[(R_P^{-1} + R_S^{-1})\,(C_P + C_S)^{-1}\,(t' - t)]\},$$

$$R_L C_L \ll R_P C_P. \tag{73}$$

Only if $\tau \gtrsim R_P C_P \approx 10^4 s \gg R_L C$, does the second term in (73) give a non-negligible contribution. Therefore retention of only the first term in (73), which would result in equation (25), yields a useful formula even when the condition $R_S C_S = R_P C_P$ does not obtain.

6. REFERENCES

[1] Edelman, S., Piezoelectric Polymer Films for Fuze Applications – Progress Report for the Period Ending December 31, 1973, Instrumentation Applications Section Report 162 (unpublished).

[2] Kawai, H., The Piezoelectricity of Poly(Vinylidene Fluoride), Japan, J. Appl. Phys. 8, pp. 975-976 (1969).

[3] Fukada, E., and Takashita, S., Piezoelectric Effect in Polarized Poly(Vinylidene Fluoride), Japan, J. Appl. Phys. 8, p. 960 (1960).

[4] Nakamura, K., and Wada, Y., Piezoelectricity, Pyroelectricity, and the Electrostriction Constant of Poly(Vinylidene Fluoride), J. Polymer Sci. A-2,9, pp. 161-173 (1971).

[5] Kittel, C., Introduction to Solid State Physics, 4th ed. (1971), p. 463, J. Wiley & Sons, N.Y.

[6] Bloomfield, P.E., Lefkowitz, I., and Aronoff, A.D., Electric Field Distributions in Dielectrics, With Special Emphasis on Near-Surface Regions in Ferroelectrics, Phys. Rev. B4, pp. 974-987 (1971).

[7] Edelman, S., Unpublished Studies of the Distribution of Piezoactivity Through a Stack of Poled Polymer Films (private communication, 1972).

[8] Mason, W.P., Piezoelectric Crystals and Their Application to Ultrasonics, pp. 36-38 (D. Van Nostrand Company, Inc., N.Y., 1960).

TABLE 1

POLING CONDITIONS, CAPACITANCE, AND PIEZOELECTRIC ACTIVITY OF 11 FOUR-SHEET BATCHES

Batch No.	31	32	33	34	36	37	38	39	43	44	45
Maximum Poling Temperature (°C)	117	107	101	111	111	119	113	120	101	104	98
Poling Voltage (V)	2000	2000	2000	2000	2000	2000	2000	2000	2250	2250	2250
Average Sheet Capacitance (nF)	13.8	13.0	12.9	14.1	13.6	13.8	13.7	13.3	13.9	13.7	13.5
Average Piezoelectric Activity (pC/N)	12.1	10.2	8.5	9.7	9.5	9.7	9.8	10.4	10.6	10.8	10.6

TABLE 2A

CAPACITANCE AND PIEZOELECTRIC ACTIVITY OF COMPONENTS
FOR FIRST INTERMEDIATE STACK OF FIFTEEN SHEETS*

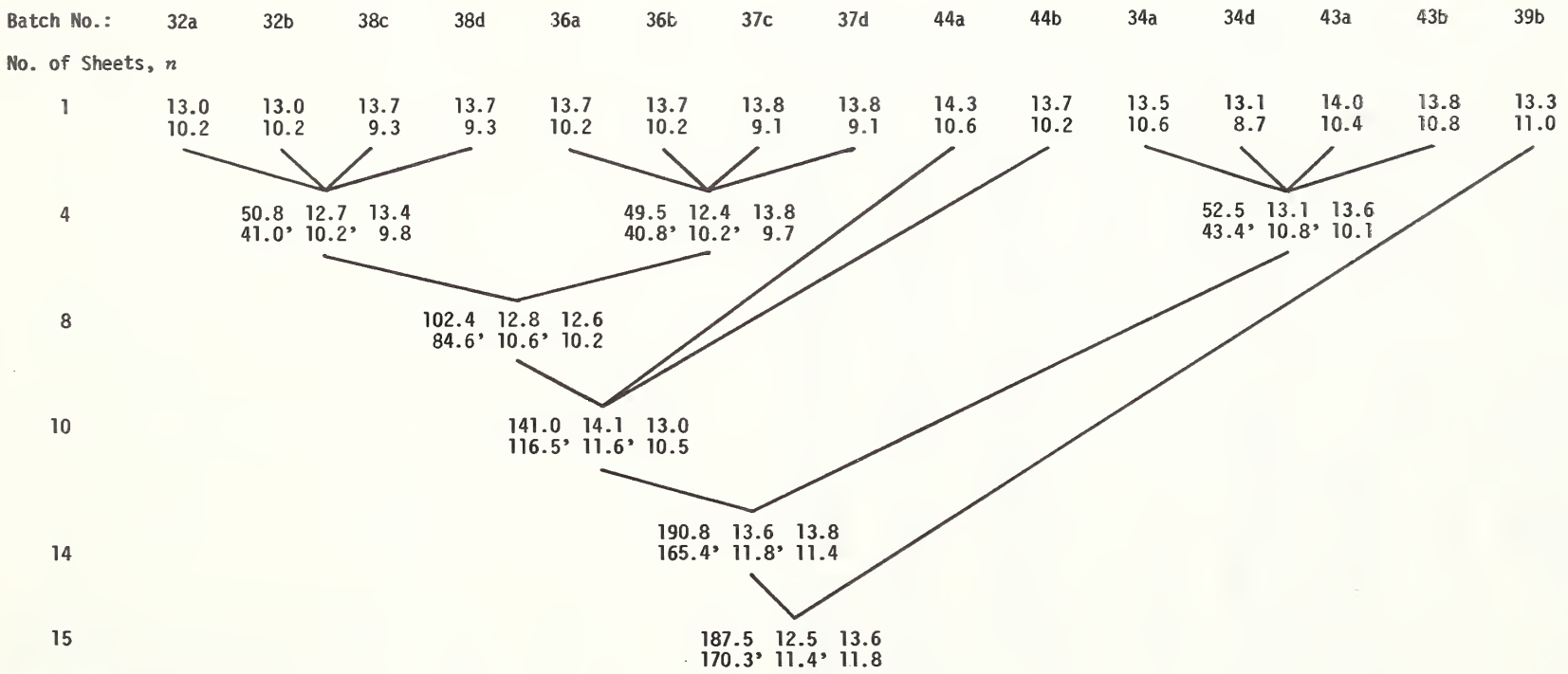

*The table is arranged in chart form to show how a fifteen-sheet stack was assembled. This stack was itself one of two intermediate stacks comprising Stack No. 7, as described in the text. For n = 1, the values of two parameters are given: the upper number is the measured sheet capacitance (nF) and the lower, the measured sheet piezoelectric activity (pC/N). For each intermediate stack, the values of six parameters are given as follows:

measured stack capacitance ,

measured stack piezoelectric activity

calculated average sheet capacitance = measured stack capacitance /n

calculated average sheet activity = measured stack activity /n

calculated average sheet capacitance based on calculated average sheet capacitance of component stacks, weighted by the number of sheets in each component ,

calculated average sheet activity based on calculated average sheet activity of component stacks, weighted by the number of sheets in each component.

TABLE 2B

CAPACITANCE AND PIEZOELECTRIC ACTIVITY OF COMPONENTS
FOR SECOND INTERMEDIATE STACK OF FIFTEEN SHEETS*

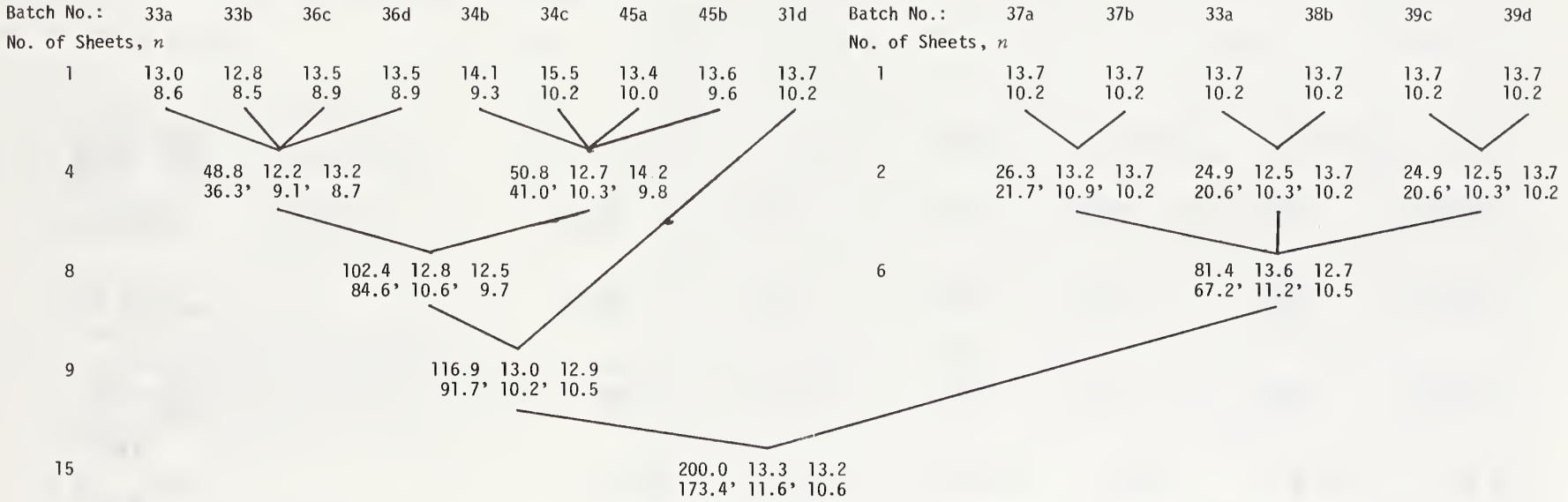

*The table is arranged in chart form to show how a fifteen-sheet stack was assembled. This stack was itself one of two intermediate stacks comprising Stack No. 7, as described in the text. For n = 1, the values of two parameters are given: the upper number is the measured sheet capacitance (nF) and the lower, the measured sheet piezoelectric activity (pC/N). For each intermediate stack, the values of six parameters are given as follows:

measured stack capacitance	calculated average sheet capacitance = measured stack capacitance /n	calculated average sheet capacitance based on calculated average sheet capacitance of component stacks, weighted by the number of sheets in each component
measured stack piezoelectric activity	calculated average sheet activity = measured stack activity /n	calculated average sheet activity based on calculated average sheet activity of component stacks, weighted by the number of sheets in each component.

Table 3

MEASURED POLYMER STACK ELECTRICAL OUTPUT PRODUCED IN RESPONSE TO IMPACT*

R_L (kΩ)	0.004	0.010	0.040	0.400	4.00	40.0
$\nu\tau \approx \tau/R_L C$	225	90.0	22.5	2.00	0.225	0.023
V_L^{MAX} [C_L = 0.5 μF] (V)	0.14	0.40	1.26	5.2	7.4	7.5
V_L^{MAX} [C_L = 15 pF]** (V)	0.15	0.40	1.33	9.6	19.4	22.5
V_L^{MIN} (V)	-0.15	-0.40	-1.33	-8.4	-4.0	0.0
$\frac{V_L^{MAX}}{F_o}$ ($\frac{\mu V}{N}$)	8.0	21.3	70.7	511	1030	1200
t_M (μs)***	100	125	125	150	200	225
t_o (μs)	225	225	250	275	375	450
$\frac{E(\tau)}{F_o^2}$ ($\frac{fJ}{N^2}$)	1.2	3.4	10.5	61.6	19.9	2.7

* The table is explained in the text.

** This C_L is the capacitance contribution of the transient recorder and is taken as the C_L for all measurements except as noted.

*** t_M = time at which $V_L = V_L^{MAX}$.

TABLE 4

COMPARISON OF CALCULATED WITH MEASURED POLYMER STACK ELECTRICAL OUTPUT PRODUCED IN RESPONSE TO IMPACT

R_L (kΩ)		0.004	0.010	0.040	0.400	4.0	40.0
$Y = \nu\tau \approx \tau/R_L C$		225	90	22.5	2	0.225	0.023
V_L^{MAX} $(\frac{\mu V}{N})$	Measured*	8.0	21.3	70.7	511	1030	1200
	Calculated**	6.9	17	69	480†	900+	1000
$\frac{\mathcal{E}(\tau)}{F_o^2}$ $(\frac{fJ}{N^2})$	Measured	1.2	3.4	10.5	61.6	19.9	2.7
	Calculated	1.3	3.3	13.4	59†	21	2.1

*Measured values are those of table 3.

**Calculated values are based on the conditions $\tau = 225$ μs, $C = 0.25$ μF, and $V_o/F_o = 1$ mV/N.

†Value calculated for $\mathcal{L}^{MAX}$ with $\nu\tau = 2.1$ ($R_L = 430$ Ω).

+Value calculated from (56), with $t = \tau$.

TABLE 5

DELIVERIES OF PIEZOID STACKS TO FRANKFORD ARSENAL IN 1974

Delivery Date	Stack Number	Sheet Thickness (μm)	Number of Sheets n	Stack Thickness (mm)	Static Capacitance (μF)	Total Activity (pC/N)	Average Sheet Activity (pC/N)
February 14	1	12	10	0.14		30	3
February 14	2	12	10	0.14		30	3
February 14	3	12	10	0.14		30	3
March 18	4	12	10	0.14		30	3
May 6	5	25	88	2.42	1.00	290	3.3
June 7	6	25	100	2.69	1.25	300	3
September 20	7	25	30	0.88	0.36	360	12
September 27	8	25	24	0.68	0.31	270	11
November 18	9	25	20	0.60	0.23	215	11
November 18	5-1Δ	25	42	1.13	0.56	145	3.4
November 18	5-2Δ	25	46	1.24	0.55	145	3.2
November 18	6-1Δ	25	56	1.52	0.68	150	2.6
November 18	6-2Δ	25	44	1.19	0.50	115	2.7
December 10	10	25	20	0.58	0.22	235	12

ΔStacks Nos. 5 and 6 were returned to NBS for repair because the tin foil leads had broken off during static testing after delivery. Each of the two stacks was split approximately in half and new leads were attached to the resulting four stacks.

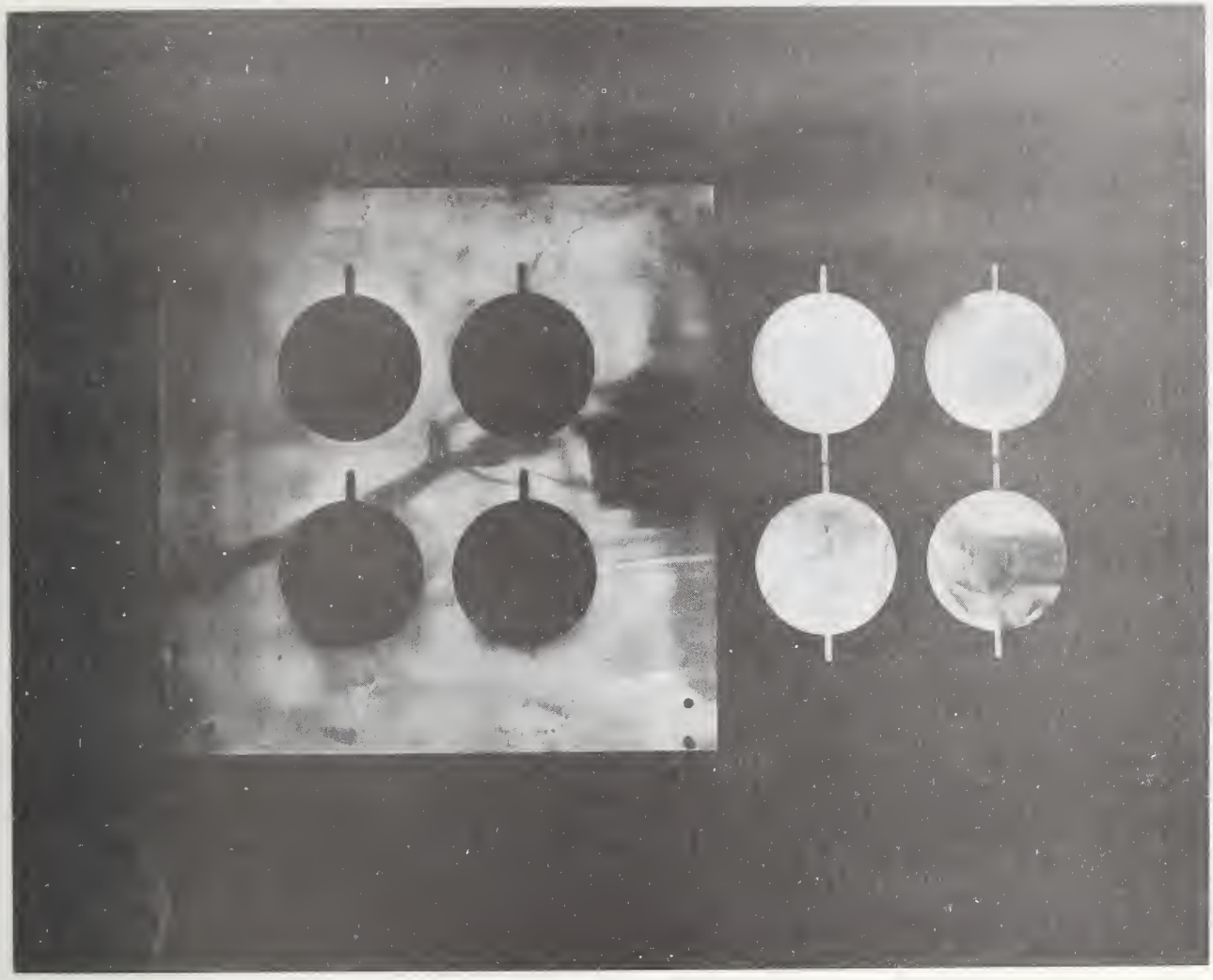

FIGURE 1: MASK AND RESULTING ELECTRODES ON PVF_2 FILM. ON THE LEFT IS THE 24-CM-SQUARE STAINLESS-STEEL MASK USED IN THE VACUUM DEPOSITION OF ALUMINUM ELECTRODES ONTO THE POLYMER SHEET MATERIAL. ON THE RIGHT ARE FOUR ELECTRODED AND POLED ACTIVE ELEMENTS. FOR EACH PIEZOID, THE TAIL SEEN AT THE BOTTOM FORMS PART OF THE UPPER ELECTRODE AND THE TAIL SEEN AT THE TOP FORMS PART OF THE LOWER ELECTRODE (HIDDEN BY THE UPPER ELECTRODE IN THE PHOTOGRAPH).

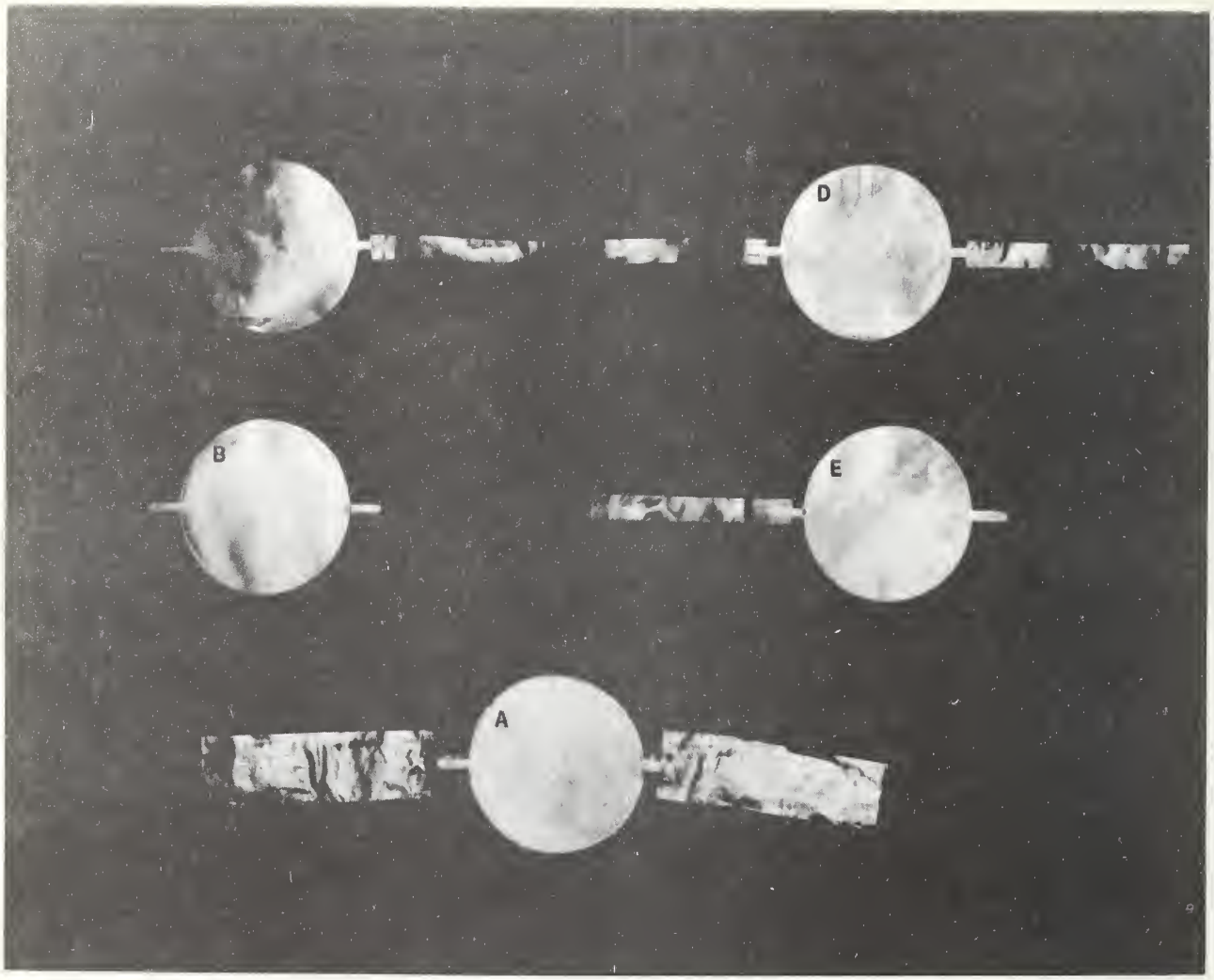

FIGURE 2: STACK CONSTRUCTION. AT THE BOTTOM (A) IS A COMPLETED STACK. THE OTHER STAGES SHOWN ARE (B) A SINGLE-SHEET PIEZOID ELEMENT, (C) A SINGLE SHEET WITH ONE FOIL ELECTRODE LEAD ATTACHED, (D) TWO SHEETS BONDED TOGETHER WITH THE HIGH-SIDE LEAD BETWEEN THE SHEETS (AT LEFT) AND TWO LOW-SIDE LEADS ATTACHED TO THE SHEET OUTER SURFACES (AT RIGHT), AND (E) TWO SHEETS BONDED TOGETHER WITH AN INTERIOR HIGH-SIDE LEAD.

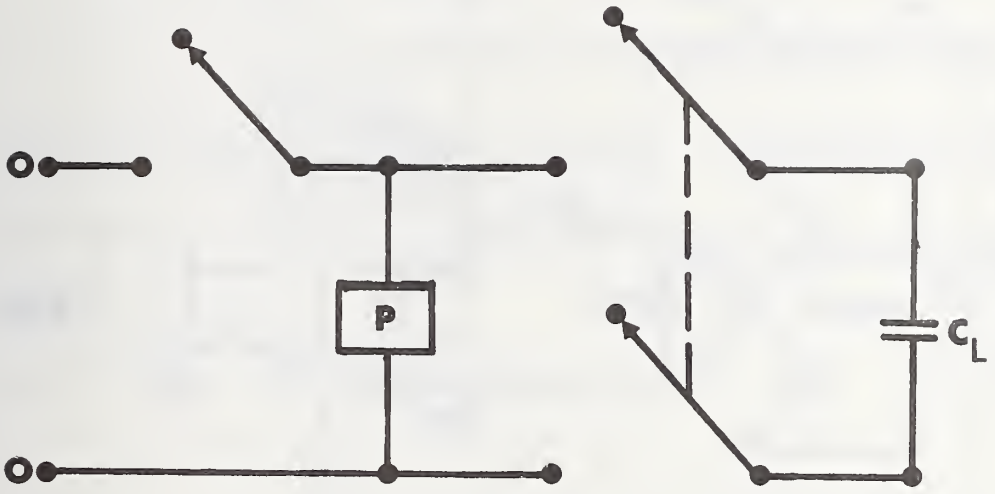

FIGURE 3: CIRCUIT USED IN STATIC-TESTING PROCEDURE. STORAGE OSCILLOSCOPE VERTICAL-AXIS INPUTS ARE MARKED O; P IS THE PIEZOID TO WHICH FORCE F_o IS APPLIED; AND C_L IS THE STANDARD CAPACITOR, AS DESCRIBED IN THE TEXT.

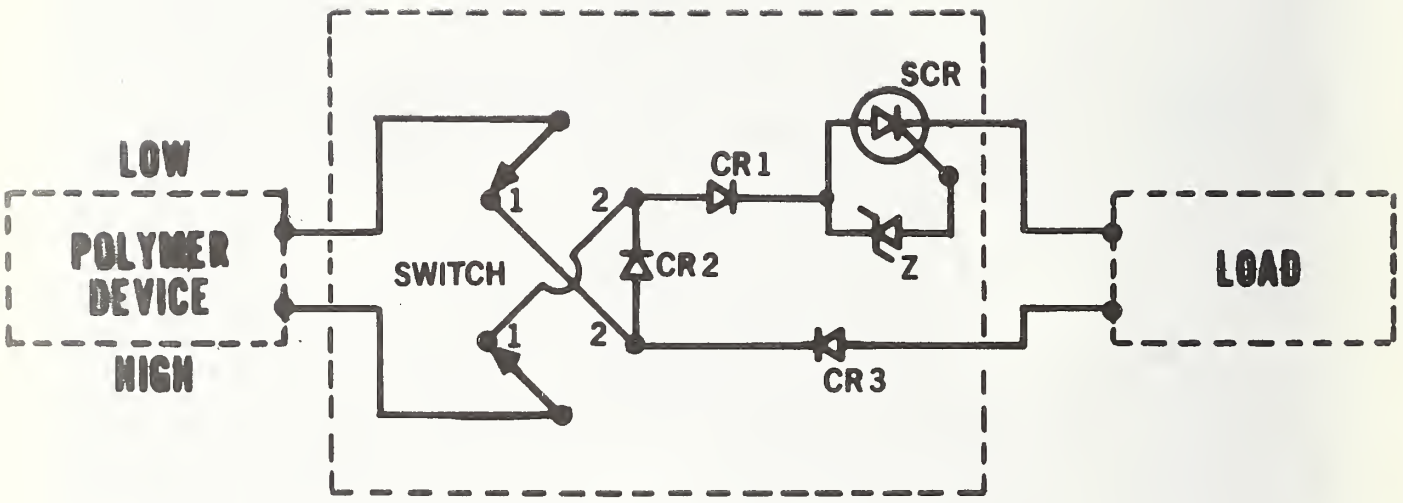

FIGURE 4: CIRCUIT USED TO CONNECT POLYMER DEVICE TO LOAD. "LOW" AND "HIGH" REFER TO POLARITIES ESTABLISHED AT THE TIME OF POLING; "HIGH" CORRESPONDS TO POSITIVE.

FOR COMPRESSION TESTS, THE DOUBLE-POLE, DOUBLE-THROW SWITCH IS IN THE POSITION SHOWN, AND THE LOW SIDE BECOMES CHARGED POSITIVELY WITH RESPECT TO THE HIGH SIDE. WHEN THE VOLTAGE SENSED BY THE ZENER DIODE REACHES THE ZENER REFERENCE VOLTAGE, THE POLYMER DEVICE DISCHARGES THROUGH DIODE CR2 INTO THE LOAD. FOR TENSION TESTS, THE SWITCH IS THROWN TO POSITION 2, AS THE DEVICE POLARITIES ARE REVERSED.

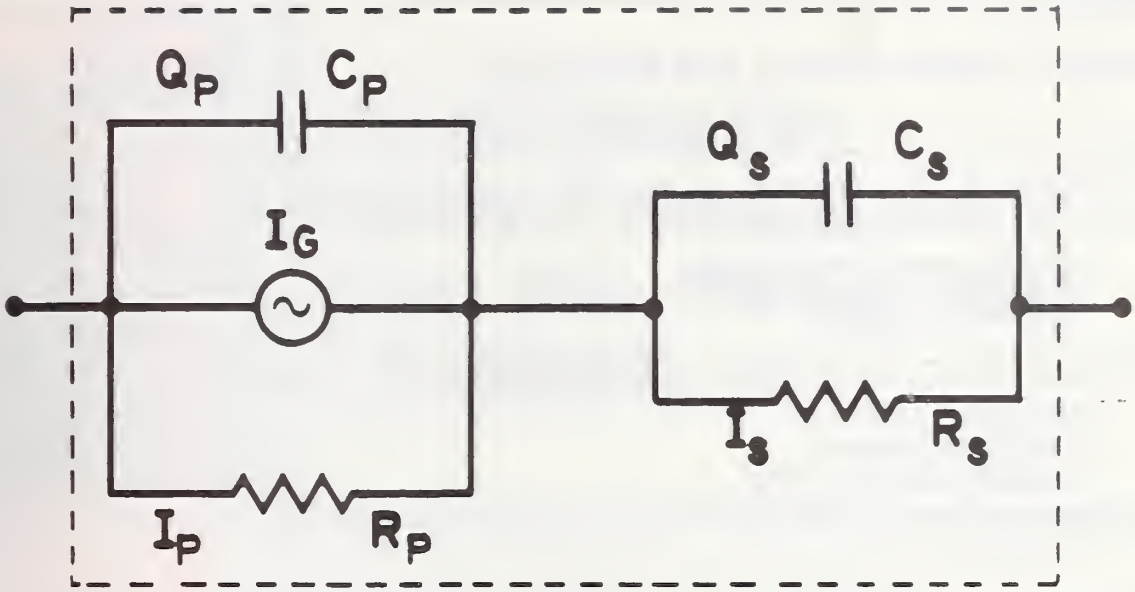

FIGURE 5: POLYMER ELEMENT EQUIVALENT CIRCUIT.

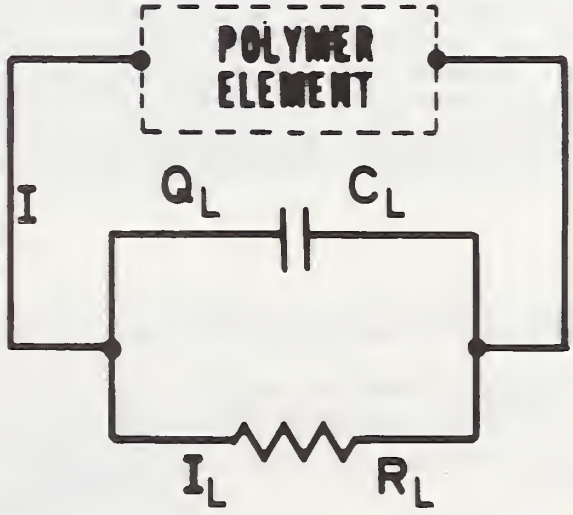

FIGURE 6: POLYMER ELEMENT CONNECTED TO ELECTRICAL LOAD.

SCOMM-NBS DC

NBS-114A (REV. 7-73)

U.S. DEPT. OF COMM. BIBLIOGRAPHIC DATA SHEET	1. PUBLICATION OR REPORT NO. NBSIR 75-724 (R)	2. Gov't Accession No.	3. Recipient's Accession No.

4. TITLE AND SUBTITLE

Piezoelectric Polymer Films for Fuze Applications

5. Publication Date: August 1975

6. Performing Organization Code: 425.03

7. AUTHOR(S): Philip E. Bloomfield

8. Performing Organ. Report No.

9. PERFORMING ORGANIZATION NAME AND ADDRESS

NATIONAL BUREAU OF STANDARDS
DEPARTMENT OF COMMERCE
WASHINGTON, D.C. 20234

10. Project/Task/Work Unit No.: 4253557

11. Contract/Grant No.: DAAA25 74 F0008

12. Sponsoring Organization Name and Complete Address *(Street, City, State, ZIP)*

U.S. Army
Frankford Arsenal
Philadelphia, PA 19137

13. Type of Report & Period Covered: Final 9/1/73 to 12/31/74

14. Sponsoring Agency Code

15. SUPPLEMENTARY NOTES

16. ABSTRACT *(A 200-word or less factual summary of most significant information. If document includes a significant bibliography or literature survey, mention it here.)*

Described is the development of polymer piezoelectric devices with sufficient electrical output in response to impact to demonstrate the feasibility of using polymer elements in place of ceramic elements in ordnance fuze systems. To satisfy this requirement, piezoelectric polymer elements have been constructed capable of providing at least 0.3 mJ into a 4-Ω load, in response to a force of 89 kN (10 tonsf). Total activities of up to 360 pC/N have been achieved from elements built up from 30 sheets of 25-μm poly(vinylidene fluoride). Test methods developed to characterize both single-sheet and total-element activities are described, as are poling procedures and details of element construction. Mathematical analyses of polymer piezoelectric output into resistive-capacitive loads are presented for static and dynamic cases. Experimental results and theoretical predictions are shown to be in agreement to within the 10% estimate of measurement accuracy.

17. KEY WORDS *(six to twelve entries; alphabetical order; capitalize only the first letter of the first key word unless a proper name; separated by semicolons)*

Calibration; electrical energy; electrical output; piezoelectric; piezoelectric output; polymer; poly(vinylidene fluoride); stack construction; theory; voltage.

18. AVAILABILITY

☐ Unlimited

☒ For Official Distribution. Do Not Release to NTIS

☐ Order From Sup. of Doc., U.S. Government Printing Office Washington, D.C. 20402, SD Cat. No. C13

☐ Order From National Technical Information Service (NTIS) Springfield, Virginia 22151

19. SECURITY CLASS (THIS REPORT)	21. NO. OF PAGES
UNCLASSIFIED	44
20. SECURITY CLASS (THIS PAGE)	22. Price
UNCLASSIFIED	